Pentafluorophenoxy Boron Subphthalocyanine As a Fluorescent Dopant Emitter in Organic Light Emitting Diodes

Michael G. Helander,[†] Graham E. Morse,[§] Jacky Qiu,[†] Jeffrey S. Castrucci,[§] Timothy P. Bender,[*,§,∥] and Zheng-Hong Lu[†,‡]

Department of Materials Science and Engineering, University of Toronto, 184 College St., Toronto, Ontario, Canada M5S 3E4, Department of Physics, Yunnan University, 2 Cuihu Beilu, Yunnan, Kunming 650091, People's Republic of China, Department of Chemical Engineering and Applied Chemistry, University of Toronto, 200 College St., Toronto, Ontario, Canada M5S 3E5, Department of Chemistry, University of Toronto, 80 St. George St., Toronto, Ontario, Canada, M5S 3H6

ABSTRACT A fluorinated phenoxy boron subphthalocyanine (BsubPc) is shown to function as a fluorescent dopant emitter in small molecule organic light emitting diodes (OLEDs). Narrow electroluminescence (EL) emission with a full width at half-maximum of ~30 nm was observed regardless of the host used, indicating that this narrow EL is intrinsic to the BsubPc molecule. A bathochromic shift and the growth of a new EL peak at higher wavelengths with increasing doping concentration were found to be a result of molecular aggregation. Excitation of BsubPc by direct charge trapping as well as Förster resonant energy transfer were shown using different host molecules. A maximum efficiency of 1.5 cd/A was achieved for a 4,4′-N,N′-dicarbazole-biphenyl (CBP) host.

KEYWORDS: boron • subphthalocyanine • light • emitting • diode • dopant • fluorescent • emitter

INTRODUCTION

Boron subphthalocyanine (BsubPc) has recently drawn interest for application in organic light emitting diodes (OLEDs) (1), organic photovoltaics (OPVs) (2), and organic thin film transistors (OTFTs) (3). BsubPc derivatives have been reported to have very narrow photoluminescence (PL) emission and quantum efficiencies near 40%, thereby making them interesting candidates as emitters in OLEDs (1a). We recently reported a series of fluorinated phenoxy-BsubPcs which exhibited extremely narrow electroluminescence (EL) emission in single layer and trilayer OLEDs (1a). The full width at half-maximum (fwhm) of our devices was only ~30 nm, whereas those of most organic emitters are ~100 nm. This fwhm is nearly half of that reported by for the only other BsubPc-based OLED reported in the literature (BsubPc as the emitter) (1d). At the time, we hypothesized that the significant difference between the EL emission reported by Diaz et al. and our results was due the difference in device architectures. Diaz et al. utilized BsubPc as a fluorescent emitter doped into a wide band gap polymer layer, whereas our devices used BsubPc as a neat film. Molecular aggregation in our neat films may have contributed to the narrow EL emission. Alternatively, host–dopant interactions in the doped films used by Diaz et al. may have significantly broadened their emission spectrum. In order to clarify this issue, we have studied the host–dopant interaction of BsubPc in doped molecular films. Herein, we report the use of pentafluorophenoxy-BsubPc (F_5BsubPc) as a fluorescent dopant emitter in OLEDs (Figure 1). Using a variety of different molecular host materials, we have characterized the energy transfer and emission processes of F_5BsubPc. As we will show, the spectrally narrow EL emission of F_5BsubPc is intrinsic to the material and is not a result of molecular aggregates.

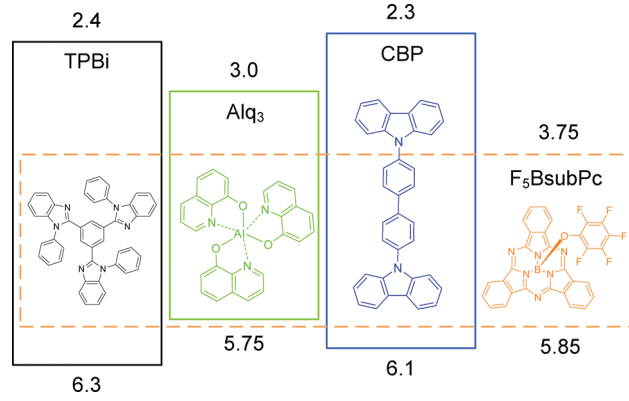

FIGURE 1. Schematic energy level diagram (from left to right) of TPBi (4), Alq_3 (4), CBP (4), and F_5BsubPc (1a) based on combined CV and UPS measurements. All energy levels are reported relative to vacuum without consideration of any interfacial dipoles. Energy levels are taken from references as indicated.

* To whom correspondence should be addressed. E-mail: tim.bender@utoronto.ca.

Received for review July 20, 2010 and accepted September 27, 2010

† Department of Materials Science and Engineering, University of Toronto.

‡ Yunnan University.

§ Department of Chemical Engineering and Applied Chemistry, University of Toronto.

∥ Department of Chemistry, University of Toronto.

DOI: 10.1021/am100632y

EXPERIMENTAL SECTION

Materials and Methods. ultraviolet−visible (UV−vis) spectroscopy was performed using a PerkinElmer Lambda 1050 in a PerkinElmer quartz cuvette with a 10 mm path length. Dimethylformamide (DMF) distilled in glass was purchased from Caledon Laboratories, Ltd. (Caledon, Ontario, Canada) and used as received. Distilled water was supplied by the Chemical Engineering Department at the University of Toronto. Photoluminescence (PL) spectra were collected using a Perkin-Elmer LS 55 in a PerkinElmer quartz cuvette with a 10 mm path length. The absorbance of each sample was measured to be >0.1 in order to avoid distortion from the inner filter effect.

Materials for OLED Fabrication. F_5BsubPc was synthesized following our previously reported method (1a) and was purified using train sublimation. Electronic grade tris-(8-hydroxy-quinolato)aluminum (Alq_3) used as a host for the emissive layer (EML) was provided by Norel Optronics, Inc. and used as received. 1,3,5-Tris(*N*-phenylbenzimidazole-2-yl)benzene (TPBi) used as an electron transport layer (ETL) and as a host for the EML and 4,4′-N,N′-dicarbazole-biphenyl (CBP) used as a hole transport layer (HTL) and as a host for the EML were purchased from Luminescence Technology Corp. and used as received. High purity (99.99% trace metals basis) LiF and MoO_3 were purchased from Sigma-Aldrich and were thoroughly degassed in high vacuum prior to use.

OLED Fabrication and Characterization. OLEDs were fabricated in a Kurt J. Lesker LUMINOS cluster tool (base pressure of $\sim 1 \times 10^{-8}$ Torr) using stainless steel shadow masks to define the device structure. Commercially patterned indium tin oxide (ITO) coated glass (50×50 mm^2) with a sheet resistance less than 15 Ω/□ was used for all devices in this study. Substrates were ultrasonically cleaned with a standard regimen of Alconox, acetone, and methanol followed by UV ozone treatment for 15 min. The standard device structure is as follows: ITO/MoO_3 (1 nm)/CBP (45 nm)/EML (15 nm)/TPBi (30 nm)/LiF (1 nm)/Al (100 nm). The different EMLs used were neat F_5BsubPc, Alq_3, CBP, and TPBi doped with F_5BsubPc at various concentrations. The doped EMLs were produced by codeposition of the host and dopant. All doping concentrations are reported in weight percent of the dopant in the host. The various organic molecules were deposited from alumina crucibles (K-cells) in a dedicated organic chamber. LiF and MoO_3 were also deposited in the same chamber from alumina crucibles. The Al cathode lines (2 mm wide) were deposited orthogonally to the ITO anode lines (1 mm wide) from a pyrolytic boron nitride crucible, in a separate metallization chamber without breaking vacuum. Film thicknesses were monitored using a calibrated quartz crystal microbalance. The intersection of each cathode and anode line yields one OLED pixel, with 32 devices per substrate. The active area for all devices was 2 mm^2. A total of up to eight different device structures were fabricated on a single substrate to eliminate possible run-to-run variability caused by subtle variations in process conditions. Current−voltage (*IV*) characteristics of the OLEDs were measured using an HP4140B pA meter in ambient air. Luminance measurements were taken using a Minolta LS-110 Luminance meter. EL spectra were measured using an Ocean Optics USB2000 fiber spectrometer with a bare optical fiber.

RESULTS AND DISCUSSION

A. Host and Dopant Properties. The selection of a suitable host material for fluorescent emitters requires careful matching of the energy levels, transport properties, and overlap of the emission and absorption spectra of the host and dopant. Excitation of a dopant emitter typically occurs through one of two processes: (i) direct carrier trapping on the dopant or (ii) Förster resonant energy transfer (FRET).

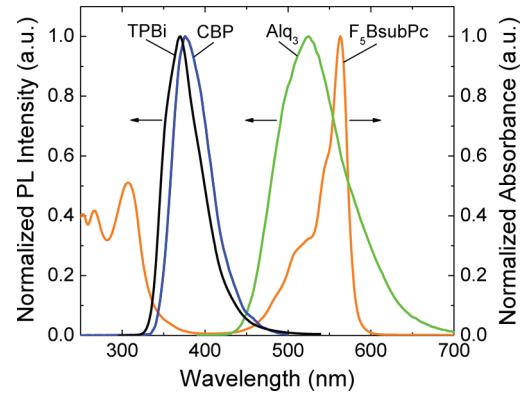

FIGURE 2. Solution PL spectra of (a) Alq_3, (b) CBP, and (c) TPBi overlaid with the absorption spectrum of F_5BsubPc in dichloromethane.

In the case of direct carrier trapping, the energy levels of the dopant should fall within the highest occupied molecular orbital (HOMO)−lowest unoccupied molecular orbital (LUMO) gap of the host. For FRET, sufficient overlap between the emission spectrum of the host and the absorption spectrum of the dopant is required. In both cases, matching a hole transporting host with an electron transporting dopant (and vice versa) is also beneficial for maintaining carrier balance across the emissive layer (EML). We have previously shown F_5BsubPc to be preferentially electron-transporting (1a).

Figure 1 shows the energy levels of F_5BsubPc relative to the different host molecules used in this study. All energy levels are based on combined cyclic voltammetry (CV) and ultraviolet photoelectron spectroscopy (UPS) measurements and are reported relative to vacuum. The energy levels of F_5BsubPc fall nicely within the HOMO−LUMO gap of both CBP and TPBi, which suggests the possibility of direct charge trapping in these systems. Figure 2 shows the PL spectra of the various host molecules overlaid with the absorption spectrum of F_5BsubPc. Clearly, the overlap for CBP and TPBi is very small, which rules out FRET for these systems. For Alq_3, however, the overlap is quite significant, suggesting that FRET is very likely. Since the HOMO of F_5BsubPc falls outside the HOMO−LUMO gap of Alq_3, direct charge trapping is energetically unfavorable, and thus FRET should be preferred.

B. Device Design. To minimize the effect of carrier injection/transport on the device performance, we opted for a trilayer OLED design with the EML sandwiched between a hole transport layer (HTL) and an electron transport layer (ETL). The energy levels of the HTL and ETL were selected to funnel carriers into the EML without confining carriers at the HTL/EML and EML/ETL interfaces. Carrier accumulation at these interfaces is known to quench excitons (4), and thus we were careful to limit this effect by choosing appropriate HTL and ETL molecules. Since carrier accumulation is dependent on the barrier height at the interface, we wanted to eliminate any barriers for all of the different host molecules. That way, we can rule out exciton quenching as contributing to any observed differences in performance of the different host molecules. Figures 1 and 3 show a schematic of the device structure and an energy level diagram for the devices used in this study. On the basis of the energy level diagram, it is

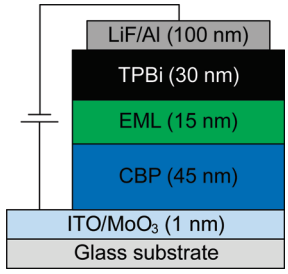

FIGURE 3. Schematic of the trilayer OLED device structure with a F_5BsubPc-based EML sandwiched between a CBP HTL and TPBi ETL. MoO_3 and LiF are used as hole injection and electron injection layers, respectively.

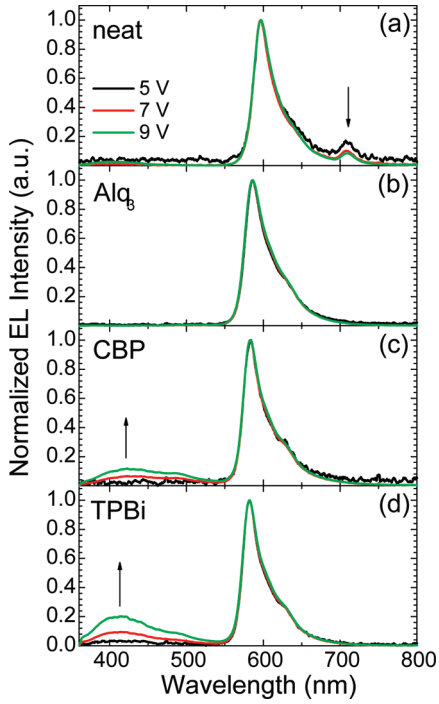

FIGURE 4. EL spectra of OLED devices as a function of applied bias with EMLs as follows: (a) neat F_5BsubPc, (b) F_5BsubPc doped into Alq_3, (c) F_5BsubPc doped into CPB, and (d) F_5BsubPc doped into TPBi.

clear that this design helps to confine carriers in the EML to maximize the probability of exciton formation and subsequent radiative recombination on the F_5BsubPc dopant.

C. Effect of Host. Figure 4 shows the EL emission spectra as a function of the applied voltage for F_5BsubPc doped into various host molecules (5 wt %) as well as for a neat film of F_5BsubPc. For the neat film of F_5BsubPc (Figure 4a), the main emission peak is centered at 601 nm (fwhm of 30 nm), with a small subpeak at 706 nm, consistent with our previous report of F_5BsubPc in single layer OLEDs (1a). The main emission peak in the doped films has the same shape and fwhm as the neat film of F_5BsubPc, but with a hypsochromic shift of 16 nm (Figure 4b–d). Also, the subpeak at ~700 nm is absent in the doped films. This suggests that the subpeak may be a result of molecular aggregates in the neat film. The difference in emission spectra between the neat and doped films will be discussed in detail in one of the following sections.

For the CPB:F_5BsubPc and TPBi:F_5BsubPc films, increasing blue emission (~400–500 nm) was observed with

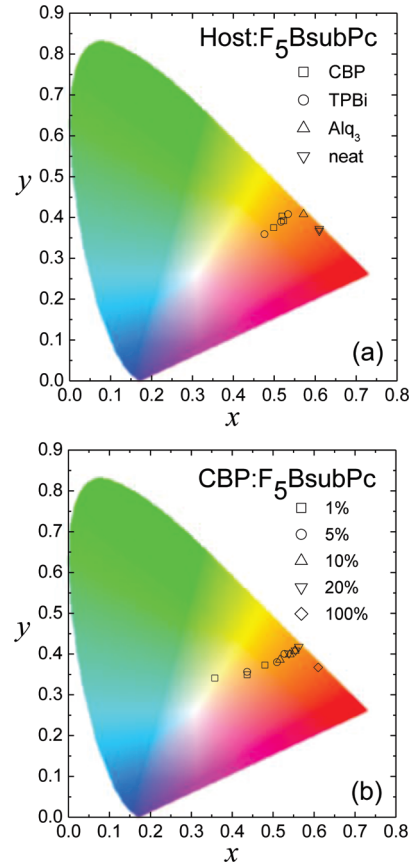

FIGURE 5. CIE coordinates of the OLED devices with F_5BsubPc doped into (a) different host molecules (CBP, TPBi, Alq_3) and (b) CBP at different doping concentrations (1%, 5%, 10%, 20%). The data for "neat" in a and 100% doping concentration in b refer to a pure F_5BsubPc film as the EML. The data for each device are shown as a function of applied voltage, with points closer to the white point corresponding to higher applied voltages.

increasing driving voltage. The position of these new emission peaks suggests that they originate from CBP and/or TPBi. It is uncertain if this blue emission is from the host or from the transport layers. Since a similar feature is also observable for the neat F_5BsubPc film, albeit much weaker and only at high applied bias (Figure 4a), it is likely that this emission originates from the transport layers due to exciton "leakage" out of the EML. For direct charge trapping, it is unlikely that all of the carriers on the host can be trapped on the dopant, particularly for low doping concentrations and high current densities. The blue emission from CBP/TPBi indicates that not all of the excitons formed in the EML are able to recombine on the F_5BsubPc dopant, which strongly suggests that excitation of the F_5BsubPc dopant occurs by direct charge trapping in these systems. Excitons that are not trapped on the F_5BsubPc dopant could "leak" out of the EML, resulting in the blue EL emission from the CBP and/or TPBi. To confirm that the blue emission is not unique to the CBP HTL, we also fabricated OLEDs using N,N′-diphenyl-N,N′-bis-(1-naphthyl)-1−1′-biphenyl-4,4′-diamine (α-NPD) as the HTL. We observed a similar blue emission at ~450 nm in these devices with increasing applied bias, which is attributed to exciton leakage to α-NPD (Supporting Information, Figure S1).

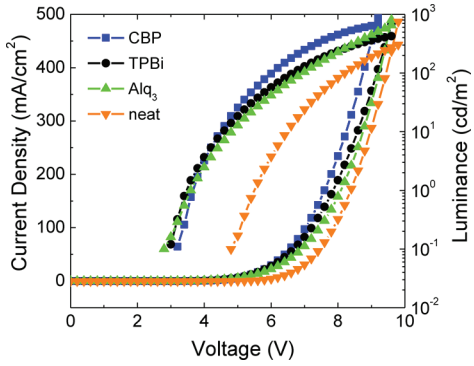

FIGURE 6. Luminance and current density as a function of voltage for OLED devices with F_5BsubPc doped into different host molecules (CBP, TPBi, Alq_3). The data for "neat" refer to a pure F_5BsubPc film as the EML.

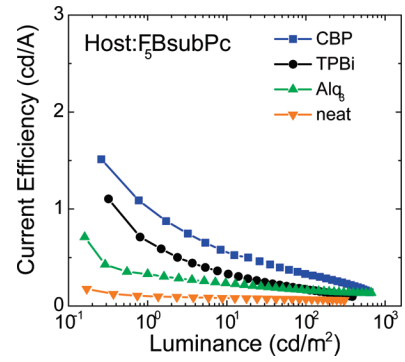

FIGURE 7. Current efficiency as a function of luminance of the OLED devices with F_5BsubPc doped into different host molecules (CBP, TPBi, Alq_3). The data for "neat" refer to a pure F_5BsubPc film as the EML.

No emission from the CBP/TPBi (ETL/HTL) layers was observed for the Alq_3:F_5BsubPc film. This finding supports our hypothesis that excitation of the F_5BsubPc in the Alq_3 host occurs by FRET, whereas direct charge trapping is the predominant mechanism for the CBP and TPBi hosts. FRET is typically a very efficient and fast energy transfer process and does not require direct contact between the host and dopant molecules, such that all of the excitons formed on the host should readily be transferred to the dopant. F_5BsubPc has a much smaller HOMO−LUMO gap than Alq_3, and hence it is energetically favorable for high energy Alq_3 excitons to transfer their energy to the lower energy excited state on the F_5BsubPc dopant. As a result, there is no exciton leakage to the HTL or ETL for the Alq_3:F_5BsubPc film, even at a high current density. The orange EL emission from the Alq_3:F_5BsubPc film is thus much more saturated than for either the CBP or TPBi hosts. Figure 5a shows the CIE coordinates of the EL emission of the various devices calculated from the EL spectra.

In our previous study, we reported a very low efficiency for F_5BsubPc single-layer OLEDs, despite a relatively high quantum efficiency of ~40% for F_5BsubPc (1a). In the present study, the efficiency of the trilayer OLED with neat F_5BsubPc film is comparable to our previously reported results. The low EL efficiency for the neat film may be due to two possible effects: (i) self-quenching and (ii) poor charge balance in the EML. We expect that both mechanisms contribute to the lower efficiency of the devices with neat F_5BsubPc as the EML.

Figure 6 shows the current density and luminance as a function of voltage for the same OLED devices discussed above. The driving voltage (for a current density of 20 mA/cm^2) and turn-on voltage (for a luminance of 1 cd/m^2) is highest for the neat F_5BsubPc film, which indicates poor carrier transport through the F_5BsubPc layer. We previously demonstrated that F_5BsubPc is a good *n*-type conductor, but with very poor hole transport properties (1a). Given the very poor hole transporting properties of F_5BsubPc, the higher driving voltage and turn-on voltage for the neat F_5BsubPc film suggests that holes are being blocked at the CBP/F_5BsubPc interface. The efficiency is therefore very low due to the poor carrier balance as well as exciton quenching from the accumulated holes at the CBP/F_5BsubPc interface.

One advantage of using a host−dopant system for the EML is that the charge transport and emission processes can be separated onto different molecules (i.e., charge transport on the host and emission from the dopant). Not surprisingly, the driving voltage and turn-on voltage are lower for the doped devices. The driving voltage is lowest for the CBP:F_5BsubPc film. This can be explained by the transport properties of the hosts. CBP is a good hole transporter, while TPBi and Alq_3 are good electron transporters (5). Since F_5BsubPc is a good electron transporter, the CBP:F_5BsubPc film has the best ambipolar transport properties and, therefore, lowest driving voltage. The ambipolar transport properties of the CBP:F_5BsubPc film are also expected to lead to the best carrier balance in the EML and, thus, the highest device efficiency. Figure 7 shows the current efficiency as a function of luminance for the same OLED devices. Indeed, the performance of the CBP:F_5BsubPc film is highest with a maximum efficiency of 1.1 cd/A at device turn-on (1 cd/m^2). This represents an increase in efficiency of ~2 orders of magnitude over the neat F_5BsubPc film (as well as our previously reported results). Clearly, BsubPc performs much better as a fluorescent dopant than as a neat emitter layer.

D. Effect of Doping Concentration. After determining that CBP is the best host for F_5BsubPc (due to the ambipolar transport properties) on the basis of the device efficiency, we studied the effect of doping concentration on the EL emission and device performance. As discussed above, there is strong evidence that the excitation process in the CBP:F_5BsubPc film occurs by direct carrier trapping on the F_5BsubPc dopant. As a result, significant exciton leakage to the HTL and/or ETL was observed in the CBP:F_5BsubPc films at a high applied bias, as indicated by intense blue emission from CBP/TPBi. If the excitation process in the CBP:F_5BsubPc film does indeed occur by direct carrier trapping, this exciton leakage should be suppressed by increasing the dopant concentration. At higher dopant concentrations, there are more F_5BsubPc molecules available to trap charges, and hence less excitons can leak out of the EML.

Figure 8 shows the EL emission spectra as a function of doping concentration for CBP:F_5BsubPc at an applied bias of 7 V. Figure 5b shows the CIE coordinates of the EL emission of the various devices calculated from the EL spectra. With increasing doping concentration, the EL emis-

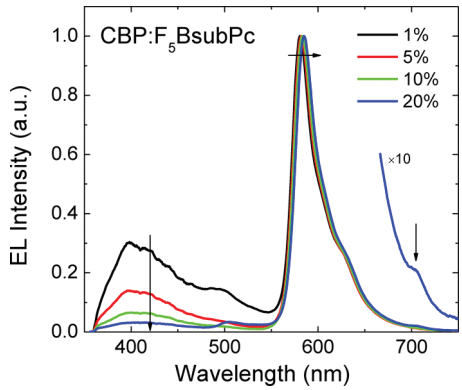

FIGURE 8. EL emission of the OLED devices with F_5BsubPc doped into CBP at different doping concentrations (1%, 5%, 10%, 20%). All values are reported in wt % of F_5BsubPc in CBP.

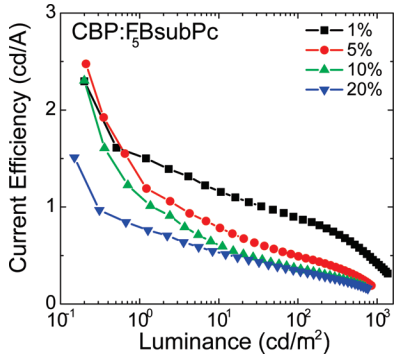

FIGURE 9. Current efficiency as a function of luminance of the OLED devices with F_5BsubPc doped into CBP with different doping concentrations (1%, 5%, 10%, 20%). All values are reported in wt % of F_5BsubPc in CBP.

sion from CBP/TPBi at ~400−500 nm is found to decrease in intensity. At the same time, there is a 5 nm bathochromic shift in the F_5BsubPc emission peak for increasing the doping concentration from 1 % to 20 %. Also, for the highest doping concentration of 20 %, there is a subpeak in the EL emission at ~700 nm, which is very similar to the subpeak observed in the neat F_5BsubPc film. We suspect that the bathochromic shift and subpeak in the EL are a result of molecular aggregation. With increasing doping concentration, there is higher probability of aggregation between adjacent F_5BsubPc molecules.

Figure 9 shows the current efficiency as a function of doping concentration for the same OLED devices. The efficiency decreases with increasing doping concentration. This finding highlights the fine balance between charge trapping, carrier balance, and self-quenching. A higher doping concentration is desirable to maximize direct charge trapping and subsequent radiative recombination on the F_5BsubPc dopant. However, with an increasing doping concentration, the carrier balance may become imbalanced, and molecular aggregation effects start to quench the EL emission. In any event, the maximum efficiency of 1.5 cd/A at device turn-on (1 cd/m^2) for the 1 % doped CBP:F_5BsubPc film is the highest value ever reported for a BsubPc-based OLED.

E. Effect of Aggregation. In our previously reported work (1a), we observed a primary EL emission at 601 nm

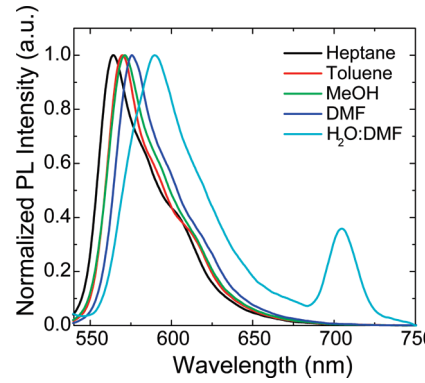

FIGURE 10. Solution PL spectra of F_5BsubPc in different solvents (as indicated).

with a low intensity secondary EL emission peak arising at 706 nm in neat thin films of F_5BsubPc. We observed a similar EL emission from the neat F_5BsubPc film used as EML in this work. Also, at high doping concentrations of F_5BsubPc in CBP, we also observed a subpeak in the EL emission around 700 nm as well as a bathochormic shift in the EL emission peak toward 600 nm. However, the peak in the solution PL measured in dichloromethane was 579 nm, while the EL emission peak in the doped films (at 5 % doping concentration) was at 585 nm. We set out to determine the root cause of these bathochromic shifts as well as the subpeak at ~700 nm. We hypothesized that these effects were a result of aggregate emission. To test this hypothesis, we initially dissolved F_5BsubPc at low concentrations in a series of poor solvents for BsubPc derivatives (methanol, heptane, and 300:1 H_2O/DMF), along with two good solvents (toluene and DMF) for comparison in an attempt to observe aggregation through changes in the PL spectrum of F_5BsubPc. Of these nonsolvents, only 300:1 H_2O/DMF had a pronounced effect on the PL spectrum (Figure 10), while bathochromic shifts of the peak PL (λ_{max}^{PL}) with increasing solvent polarity was also observed. In the case of 300:1 H_2O/DMF, the presence of a PL emission peak centered at 593 nm with a secondary emission at 706 nm (Figure 10) was observed, which is similar to features present in the EL spectrum for neat F_5BsubPc films (Figure 4a).

Interested in exploring this aggregation, we sequentially changed the ratios of water and DMF from pure DMF to 300:1 (H_2O/DMF) while maintaining a constant concentration of F_5BsubPc. In pure DMF, the main PL peak was at 576 nm (Figure 11a). As water was introduced at a 1:1 and a 3:1 H_2O/DMF ratio, the PL maximum shifted to 581 nm. Further dilution to a 4:1 ratio resulted in simultaneous emissions at 581 and 593 nm, with the latter becoming the sole emission at ratios of 8:1 and 64:1. Simultaneously, the absorption spectra of F_5BsubPc showed an absorption maximum (λ_{max}) at 568 nm for ratios of 1:1 and 3:1 (consistent with the λ_{max} for absorption spectra of F_5BsubPc in good solvents) with the onset of a new absorption band at 587 nm and a shoulder at 576 nm for ratios between 5:1 and 64:1 (Figure 12). Further dilution between 128:1 and 300:1 displayed a simultaneous PL emission at 706 nm (Figure 11c), the intensity of which increased at higher concentrations of water. This suggests

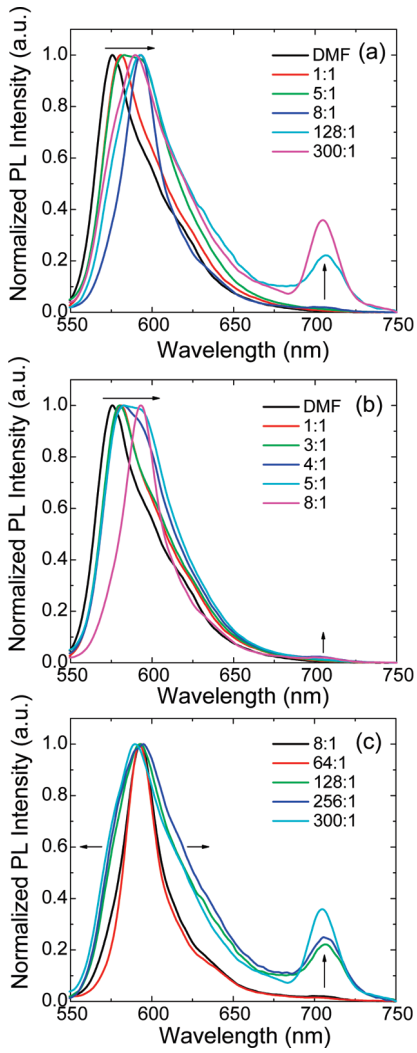

FIGURE 11. Solution PL spectra of F_5BsubPc in different ratios of H_2O/DMF (as indicated).

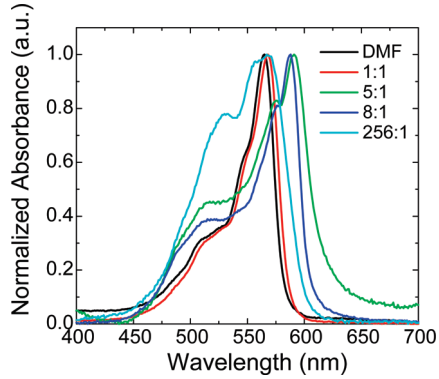

FIGURE 12. Solution absorption spectra of F_5BsubPc in different ratios of H_2O/DMF (as indicated).

that the root cause of the emission is from larger aggregates which have formed in solution. At high concentrations of water, the absorption spectrum had a λ_{max} at 567 nm similar to that in pure DMF but was broadened, as you would expect from aggregation (Figure 12). In summary, the emission of F_5BsubPc is effected by aggregation causing a bathochromic shift from 579 to 593 nm with increasing aggregation. A secondary emission in the PL centered at 706 nm begins to form with increasing aggregation, verifying that the emissions observed in the EL spectra of neat F_5BsubPc films (or at high doping concentrations) near 600 and 700 nm are emissions arising from these aggregates.

CONCLUSION

F_5BsubPc has been demonstrated as a fluorescent dopant emitter in OLEDs. The efficiency of devices with F_5BsubPc doped into a wide band gap host molecule was 2 orders of magnitude higher than for neat films of F_5BsubPc. Using CBP as the host, a maximum efficiency of 1.5 cd/A was achieved with highly saturated orange EL, the highest ever reported for a BsubPc-based OLED. The EL spectra of neat F_5BsubPc exhibited a bathochromic shift relative to the doped devices and a subpeak to higher wavelength. These phenomena were found to be a result of molecular aggregation in the neat films. Similar features were also observed at high doping concentrations. It was also determined that excitation of F_5BsubPc occurs by direct carrier trapping in CBP and TPBi hosts, and by FRET in an Alq_3 host. The previously reported narrow EL emission (fwhm of ~30 nm) was preserved in all devices, indicating that the narrow EL is not due to molecular aggregates but rather is intrinsic to the BsubPc molecule.

Acknowledgment. We wish to acknowledge funding for this research from Natural Sciences and Engineering Research Council (NSERC) of Canada.

Supporting Information Available: EL spectra as a function of the voltage of devices with a traditional α-NPD HTL (PDF). This material is available free of charge via the Internet at http://pubs.acs.org.

REFERENCES AND NOTES

(1) (a) Morse, G. E.; Helander, M. G.; Maka, J. F.; Lu, Z. H.; Bender, T. P. *ACS Appl. Mater. Interfaces* **2010**, in press. (b) Chen, Y. H.; Chang, Y. J.; Lee, G. R.; Chang, J. H.; Wu, I. W.; Fang, J. H.; Hsu, S. H.; Liu, S. W.; Wu, C. I.; Pi, T. W. *Org. Electron.* **2010**, *11*, 445–449. (c) Chen, Y. H.; Chang, J. H.; Lee, G. R.; Wu, I. W.; Fang, J. H.; Wu, C. I. *Appl. Phys. Lett.* **2009**, *95*, 133302. (d) Díaz, D. D.; Bolink, H. J.; Cappelli, L.; Claessens, C. G.; Coronado, E.; Torres, T. *Tetrahedron Lett.* **2007**, *48*, 4657–4660.

(2) (a) Mutolo, K. L.; Mayo, E. I.; Rand, B. P.; Forrest, S. R.; Thompson, M. E. *J. Am. Chem. Soc.* **2006**, *128*, 8108–8109. (b) Gommans, H.; Cheyns, D.; Aernouts, T.; Girotto, C.; Poortmans, J.; Heremans, P. *Adv. Funct. Mater.* **2007**, *17*, 2653–2658. (c) Gommans, H.; Aernouts, T.; Verreet, B.; Heremans, P.; Medina, A.; Claessens, C. G.; Torres, T. *Adv. Funct. Mater.* **2009**, *19*, 3435–3439. (d) Kumar, H.; Kumar, P.; Bhardwaj, R.; Sharma, G. D.; Chand, S.; Jain, S. C.; Kumar, V. *J. Phys. D: Appl. Phys.* **2009**, *42*, 015103. (e) Ma, B.; Woo, C. H.; Miyamoto, Y.; Frechet, J. M. J. *Chem. Mater.* **2009**, *21*, 1413–1417. (f) Klaus, D.; Knecht, R.; Dragässer, A.; Keil, C.; Schlettwein, D. *Phys. Status Solidi A* **2009**, *206* (12), 2723–2730. (g) Ma, B.; Miyamoto, Y.; Woo, C. H.; Fréchet, J. M. J.; Zhang, F.; Liu, Y. *Proc. SPIE* **2009**, *7416*, 74161E–1.

(3) (a) Yasuda, T.; Tsutsui, T. *Mol. Cryst. Liq. Cryst.* **2007**, *462*, 3–9. (b) Renshaw, K. C.; Xu, X.; Forrest, S. R. *Org. Electron.* **2010**, *11*, 175–178.

(4) (a) Wang, Z. B.; Helander, M. G.; Liu, Z. W.; Greiner, M. T.; Qiu, J.; Lu, Z. H. *Appl. Phys. Lett.* **2010**, *96* (4), 043303−3. (b) Wang, Z. B.; Helander, M. G.; Qiu, J.; Liu, Z. W.; Greiner, M. T. Z. H. *J. Appl. Phys.* **2010**, *108* (2), 024510−4.

(5) (a) Koene, B. E.; Loy, D. E.; Thompson, M. E. *Chem. Mater.* **1998**, *10*, 2235–2250. (b) Shi, J.; Tang, C. W.; Chen, C. H. U.S. Patent 5.645,948, Jul 8, 1997. (c) Tang, C. W.; VanSlyke, S. A. *Appl. Phys. Lett.* **1987**, *51* (12), 913–915.

AM100632Y